

# UC Berkeley

## UC Berkeley Previously Published Works

### Title

A Long-Life, High-Rate Lithium/Sulfur Cell: A Multifaceted Approach to Enhancing Cell Performance

### Permalink

<https://escholarship.org/uc/item/97z815sv>

### Journal

Nano Letters, 13(12)

### ISSN

1530-6984

### Authors

Song, Min-Kyu  
Zhang, Yuegang  
Cairns, Elton J

### Publication Date

2013-12-11

### DOI

10.1021/nl402793z

Peer reviewed

# A Long-Life, High-Rate Lithium/Sulfur Cell: A Multifaceted Approach to Enhancing Cell Performance

Min-Kyu Song,<sup>†,‡</sup> Yuegang Zhang,<sup>\*,†,§</sup> and Elton J. Cairns<sup>\*,†,||</sup>

<sup>†</sup>The Molecular Foundry, Lawrence Berkeley National Laboratory, Berkeley, California 94720, United States

<sup>‡</sup>Department of Chemical and Biomolecular Engineering, University of California, Berkeley, California 94720, United States

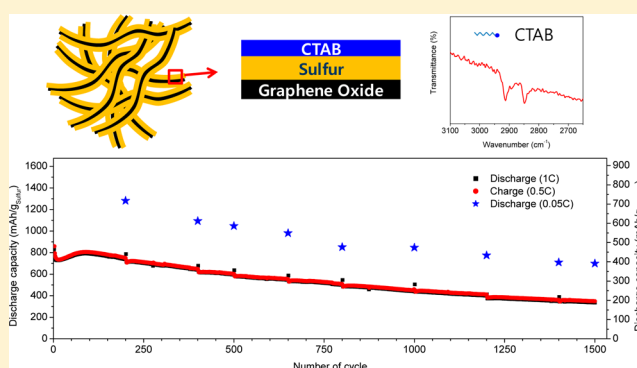
<sup>§</sup>i-LAB, Suzhou Institute of Nano-Tech and Nano-Bionics, Chinese Academy of Sciences, Suzhou 215123, China

<sup>||</sup>Environmental Energy Technologies Division, Lawrence Berkeley National Laboratory, Berkeley, California 94720, United States

## S Supporting Information

**ABSTRACT:** Lithium/sulfur (Li/S) cells are receiving significant attention as an alternative power source for zero-emission vehicles and advanced electronic devices due to the very high theoretical specific capacity (1675 mA·h/g) of the sulfur cathode. However, the poor cycle life and rate capability have remained a grand challenge, preventing the practical application of this attractive technology. Here, we report that a Li/S cell employing a cetyltrimethyl ammonium bromide (CTAB)-modified sulfur-graphene oxide (S-GO) nanocomposite cathode can be discharged at rates as high as 6C (1C = 1.675 A/g of sulfur) and charged at rates as high as 3C while still maintaining high specific capacity (~800 mA·h/g of sulfur at 6C), with a long cycle life exceeding 1500 cycles and an extremely low decay rate (0.039% per cycle), perhaps the best performance demonstrated so far for a Li/S cell. The initial estimated cell-level specific energy of our cell was ~500 W·h/kg, which is much higher than that of current Li-ion cells (~200 W·h/kg). Even after 1500 cycles, we demonstrate a very high specific capacity (~740 mA·h/g of sulfur), which corresponds to ~414 mA·h/g of electrode: still higher than state-of-the-art Li-ion cells. Moreover, these Li/S cells with lithium metal electrodes can be cycled with an excellent Coulombic efficiency of 96.3% after 1500 cycles, which was enabled by our new formulation of the ionic liquid-based electrolyte. The performance we demonstrate herein suggests that Li/S cells may already be suitable for high-power applications such as power tools. Li/S cells may now provide a substantial opportunity for the development of zero-emission vehicles with a driving range similar to that of gasoline vehicles.

**KEYWORDS:** Energy storage, lithium batteries, sulfur, graphene oxides, cathodes



Air pollution and global warming cannot be neglected anymore, and the total global energy consumption is expected to double in upcoming decades. There has therefore been strong demand for sustainable, clean energy technologies. Among many available energy storage devices, rechargeable Li-ion batteries still represent the state-of-the-art technology in the market.<sup>1–6</sup> However, there is a key challenge which must be overcome; current Li-ion batteries are not able to meet the ever-increasing demands of advanced technologies and the need for lower cost. For example, the energy-storage capacity of batteries must be dramatically improved to increase the driving range of current electric vehicles.<sup>7</sup> For the development of advanced electric vehicles that can provide ~300 mi range, the battery should provide a cell-level specific energy of 350–400 W·h/kg. This would require almost double the specific energy (~200 W·h/kg) of current lithium-ion batteries. In addition, the cycle life must be improved to more than 1000 cycles,<sup>8,9</sup> preferably up to 1500 cycles, and a rate performance greater

than 2C would be necessary to provide a peak power of ~600 W/kg or higher.

Recently, lithium/sulfur (Li/S) cells have gained intense attention because they have a much higher theoretical specific energy (~2600 W·h/kg) than that of current lithium-ion cells (~600 W·h/kg).<sup>10–19</sup> This is due to the very high specific capacity of sulfur (1675 mA·h/g), based on a two-electron reaction ( $S + 2Li^+ + 2e^- \leftrightarrow Li_2S$ ), which is significantly larger than the specific capacities of current cathode materials (130–200 mA·h/g). It is expected that advanced Li/S cells could provide a driving range for electric vehicles of greater than 300 mi.<sup>10</sup> In addition, sulfur is inexpensive, abundant on earth, and environmentally benign. However, there is a critical challenge in the development of advanced Li/S cells.

Received: July 26, 2013

Revised: November 9, 2013

When elemental sulfur reacts with lithium ions to form  $\text{Li}_2\text{S}$ , intermediate species (e.g.,  $\text{Li}_2\text{S}_8$ ,  $\text{Li}_2\text{S}_6$ ,  $\text{Li}_2\text{S}_4$ ) are formed, and these lithium polysulfides are soluble in most organic electrolyte solutions. This high solubility can lead to the loss of active material (i.e., sulfur) from the positive electrode during operation, which is a major contributor to the fast capacity fading upon cycling. When these lithium polysulfides are formed and dissolved in the electrolyte solution, they can diffuse to the lithium metal electrode and form insoluble  $\text{Li}_2\text{S}_2$  and/or  $\text{Li}_2\text{S}$  on its surface. The lithium polysulfides can also shuttle back and forth between negative and positive electrodes, lowering the Coulombic efficiency of Li/S cells.<sup>20</sup> The conversion reaction ( $\text{S} \leftrightarrow \text{Li}_2\text{S}$ ) also involves  $\sim 76\%$  volume expansion/contraction during operation, which can lead to the cracking or disintegration of electrodes and severe capacity fading upon cycling.

Therefore, it is very important to recognize that the cycle life of Li/S cells is limited by coupled “chemical” and “mechanical” degradations.<sup>11</sup> Both degradation mechanisms must be properly addressed to dramatically improve current-technology Li/S cells. The approach of improving a single component, however, may not allow us to address all of the issues that are interlinked.<sup>11,21</sup> A more holistic research approach is needed to address these complex, interlinked problems in order to radically extend the cycle life and performance of Li/S cells. To address these difficult issues, in addition to the efforts targeting the understanding of how to control each material’s functionalities at the component level, scientific approaches for effectively linking these constituent materials together must be taken to produce systems that function synergistically on much larger scales in order to achieve unparalleled performance.

In addition, the insulating nature of sulfur and the  $\text{Li}_2\text{S}$  discharge product limits high-rate operation. Furthermore, the charging time for this battery technology must be reduced significantly to be considered as a practical alternative for gasoline-fueled vehicles in the market. Due to the low electronic conductivity of sulfur, a large amount of electronically conductive material must be employed in the electrode, which can often offset the merit of this technology, that is, high specific energy. Although the capacity in the literature is very high when normalized by the weight of sulfur only, the specific capacity based on total electrode mass is typically lower than 600 mA·h/g (of electrode) and sometimes even lower than 400 mA·h/g (of electrode), which is just equivalent to that of current Li-ion batteries.<sup>11</sup> Therefore, the sulfur content and loading must be increased, while maintaining high utilization and obtaining long cycle life, to fully harness the potential of the Li/S chemistry.

Here we report a long-life, high-rate Li/S cell with a high specific energy that exploits the unique combination of a cetyltrimethyl ammonium bromide (CTAB)-modified sulfur-graphene oxide (S-GO) nanocomposite cathode fabricated with elastomeric styrene butadiene rubber (SBR)/carboxy methyl cellulose (CMC) binder, the new formulation of our ionic liquid-based electrolyte that contains ionic liquid, *n*-methyl-(*n*-butyl) pyrrolidinium bis(trifluoromethanesulfonyl)imide (PYR14TFSI), and a mixture of 1,3-dioxolane (DOL) and dimethoxyethane (DME) with 1 M lithium bis(trifluoromethylsulfonyl)imide (LiTFSI), and a lithium metal electrode protected by lithium nitrate ( $\text{LiNO}_3$ ) additive in the electrolyte. The Li/S cell demonstrated herein synergizes some existing concepts and presents a performance that has never been realized before. We demonstrate that Li/S cells can have

an ultralong service life exceeding 1500 cycles at the 1C rate (1.675 A/g of sulfur) with excellent specific capacity:  $\sim 846$  mA·h/g of sulfur at 0.05C after 1000 cycles at 1C and  $\sim 740$  mA·h/g of sulfur at 0.02C after 1500 cycles at 1C. We also show that a Li/S cell can be discharged at rates as high as 6C (10.05 A/g of sulfur) and charged at rates as high as 3C (5.03 A/g of sulfur), while still maintaining a specific capacity ( $\sim 800$  mA·h/g of sulfur at 6C) much higher than those (130–200 mA·h/g) of current cathode materials for Li-ion cells at much lower C-rates (typically at 0.1–0.5C).

The loss of sulfur (as polysulfides) from the positive electrode represents a grand challenge in achieving a long cycle life. To address this issue, physical adsorption approaches using a high surface area of carbons have been employed.<sup>22–28</sup> Nazar and co-workers pioneered the use of a large effective surface area of mesoporous carbon to help adsorb dissolved lithium polysulfides and therefore improve the cycling performance of Li/S cells.<sup>22</sup> Due to the weak physical adsorption in the open porous structures, however, the polysulfide dissolution problem was not completely avoided. The cycle life using this physical adsorption approach demonstrated so far is often less than 200 cycles, which is insufficient for many intended applications such as portable electronics and electric vehicles. To improve the cycling performance, we have used graphene oxide (GO) as a sulfur immobilizer.<sup>29</sup> We found that the functional groups (such as hydroxyl, epoxide, carbonyl, and carboxyl groups) on the surface of graphene oxide form bonds with sulfur.<sup>29,30</sup> Both Raman and S 2p X-ray photoelectron spectroscopic analysis showed the existence of chemical bonding between GO and sulfur after chemically depositing a thin sulfur coating onto GO.<sup>30</sup> With this chemical approach, we have successfully immobilized sulfur and lithium polysulfides via the reactive functional groups on graphene oxide.

Although our previous results showed a stable cycling performance of up to 50 deep cycles using our GO-S nanocomposite cathodes, the deterioration of capacity becomes more significant with higher loadings of sulfur under the same conditions (Figure S1). Such deterioration is the major barrier to commercialization of this technology. Possible mechanisms of such deterioration in S-GO nanocomposite cathodes are that (1) only the inner layer of sulfur is directly immobilized by the intimate contact with GO; therefore outer-layer sulfur can be dissolved into the electrolyte, and lithium polysulfides not immobilized by GO can diffuse to the opposite electrode; (2) extended cycling can still cause the disintegration of the electrode because the conventional binder (polyvinylidene fluoride, PVDF) used in previous work cannot accommodate the accumulated strain/stress induced by repeated expansion ( $\text{S} \rightarrow \text{Li}_2\text{S}$ ) and contraction ( $\text{Li}_2\text{S} \rightarrow \text{S}$ ) processes during the extended cycling. Also, the sulfur loading in the earlier work was about 67 wt % of sulfur in the S-GO nanocomposite (with 70 wt % of S-GO in the composite electrodes), which results in a low specific capacity of the sulfur electrodes.

To obtain a significantly improved cycle life, the outer layer of sulfur must first be protected from dissolving, while the inner layer of sulfur can be immobilized by the functional groups on the GO. This issue is even more critical when the sulfur loading on the GO is increased, as the coating becomes thicker, which means that a larger portion of the sulfur is vulnerable to this dissolution issue. In this work, we used CTAB-modified S-GO nanocomposite to address this issue. CTAB is one kind of cationic surfactant (Scheme S1) used to modify the surface functionality of nanoparticles (e.g., iron oxides) in drug delivery

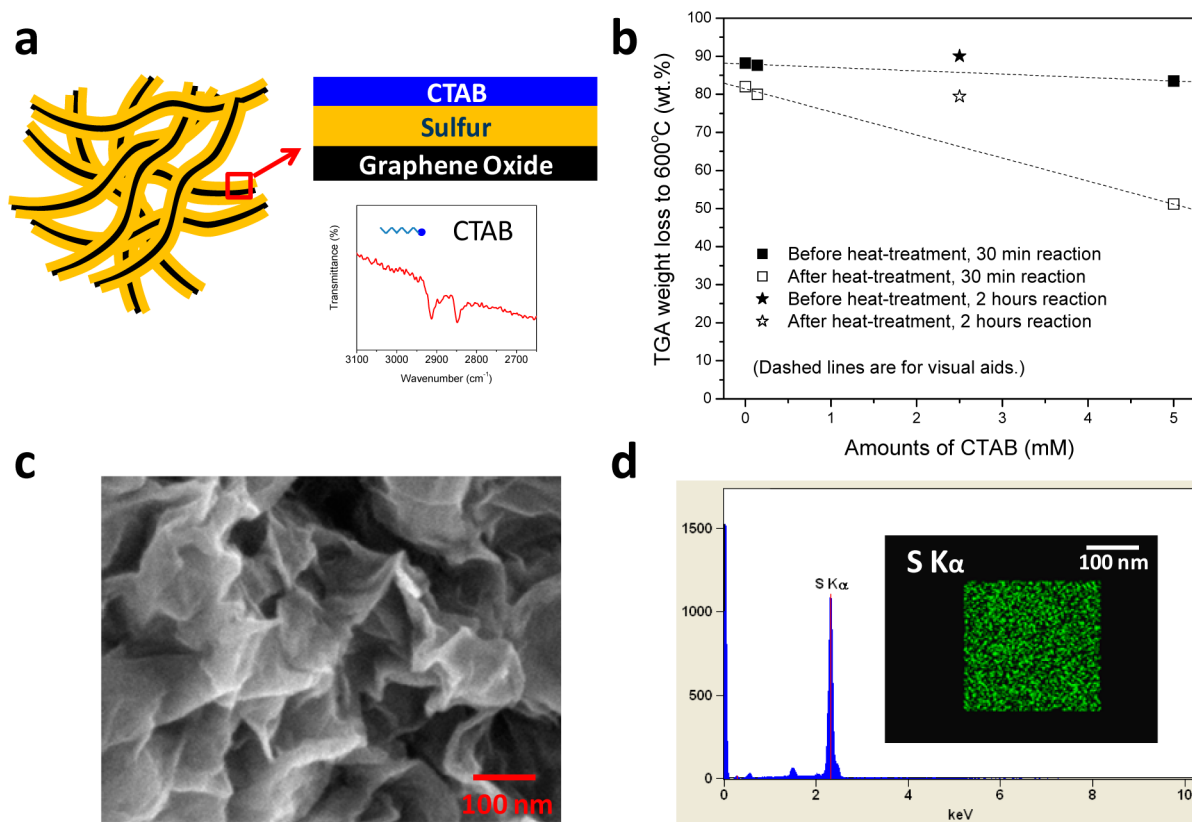


**Figure 1.** Synthesis and characterization of CTAB-modified S–GO nanocomposite. (a) Schematic of the S–GO nanocomposite structure. The presence of CTAB on the S–GO surface was confirmed by Fourier transform infrared spectroscopy (FTIR) and shown to be critical for achieving improved cycling performance by minimizing the loss of sulfur. (b) TGA weight loss of the S–GO composites as a function of the amounts of CTAB added during the synthesis of the S–GO composites. 2.5 mM CTAB and the reaction time of 2 h were chosen to achieve high sulfur content (~80%) with improved cycling performance. (c) Typical morphology of the S–GO composites examined by scanning electron microscopy. No substantial agglomeration of sulfur was observed. (d) Energy dispersive X-ray spectroscopy mapping analysis results showing the uniform deposition of a thin layer of S onto GO.

research<sup>31,32</sup> and water treatment.<sup>33–35</sup> It is well-known that the amount of CTAB can significantly affect the adsorption capability toward dyes and organic compounds when deposited onto the surface of these nanoparticles.<sup>33–35</sup> Therefore, CTAB-modified sulfur anchored on the functional groups of GO should be a significant improvement of the sulfur electrode for advanced Li/S cells. Figure 1a shows the concept of our approach.

Through a procedure developed in our laboratory, we synthesized S–GO nanocomposites with sulfur anchored on graphene oxide.<sup>29</sup> To deposit CTAB on the surface of sulfur, CTAB was added during the acidification of sodium polysulfide in formic acid for 30 min at room temperature. The amount of CTAB was varied from 0 to 5 mM in order to investigate the effect of CTAB modification on the electrochemical performance of S–GO nanocomposite cathodes. The presence of CTAB on the surface of S–GO nanocomposites was analyzed by FTIR (Figures 1a, S2) and the sulfur loading was determined by TGA (Figure S3). According to the literature,<sup>36</sup> the FTIR peaks at 2918 and 2848  $\text{cm}^{-1}$  can be attributed to two different C–H vibrational bands of CTAB, implying that the S–GO surface was well modified with CTAB. Before heat-treatment at 155 °C under Ar, the sulfur loading was not sensitive to the amount of CTAB added (average ~86%). However, after heat-treatment, we found the weight loss during TGA decreased as more CTAB was added (Figure 1b, dashed lines are for visual aid). For example, without CTAB, the

remaining sulfur (based on the TGA scan) was ~82%, but with 5 mM of CTAB, the weight loss during TGA was reduced to only ~50% after heat treatment.

Without CTAB, and with high sulfur loading (~82%), the cell capacity decreased rapidly, whereas the addition of just 0.14 mM CTAB (S ~ 80%) showed improved capacity retention (Figure S4). The addition of a larger amount of CTAB (5 mM) showed the best capacity retention. However, the improvement of cycling performance by adding CTAB was at the expense of lower S loading. To increase the sulfur loading with the presence of CTAB, 2.5 mM of CTAB was chosen, and the reaction time was increased from 30 min to 2 h. We obtained higher sulfur loading ~90% before heat treatment and ~80% sulfur loading after heat-treatment for 12 h as shown in Figure 1b.

The heat-treatment process is also critical as it allows molten sulfur to diffuse into the nanopores of GO to allow more sulfur to be immobilized by the GO matrix.<sup>22,29</sup> This could also improve the uniformity of the sulfur coating on the GO surfaces and increase utilization of sulfur. For example, when the heat-treatment time was decreased from 12 h to 30 min, higher sulfur loading (~77% sulfur with 5 mM CTAB) was obtained due to limited sulfur loss during heat-treatment, but very poor utilization was observed (Figure S5). However, with the optimized synthesis procedure, the coating of sulfur was uniform, even with 80% sulfur, which was confirmed by scanning electron microscopy (SEM) and energy dispersive X-

ray spectroscopy (EDS) mapping analysis (Figures 1c,d, S6). The typical morphology of the composites observed by scanning electron microscopy (SEM) is shown in Figure 1c. Sulfur is uniformly deposited onto graphene oxide with no substantial agglomeration of sulfur. Uniform, thin deposition of sulfur is critical to achieving high utilization and fast kinetics by providing good electron pathways with reduced diffusion length of lithium within the composites.<sup>2</sup> Indeed, CTAB-modified S-GO nanocomposite cathodes delivered a specific capacity of 1440 mA·h/g of sulfur at the 0.2C rate (1C = 1675 mA/gS), which is ~86% of the theoretical value (Figure 3a).

Raman spectroscopy was used to investigate the interaction between CTAB and sulfur. For this study, CTAB-modified sulfur nanoparticles were prepared using the same method (as described for CTAB-modified S-GO) but without adding graphene oxide (GO), as that would make it more difficult to separate carbon and hydrogen atoms from GO and CTAB. Sulfur nanoparticles were also prepared as a control sample synthesized using the same method but without adding CTAB and GO. As shown in Figure 2, the synthesized CTAB-sulfur showed the main peaks originating from sulfur. Other small peaks are from CTAB, indicating that the surface of the sulfur nanoparticles is significantly modified by CTAB. When we magnify the Raman spectra in the range from 500 to 1000  $\text{cm}^{-1}$ , it clearly shows the formation of a new peak, which can

be assigned as a C-S bond ( $600\text{--}700\text{ cm}^{-1}$ ). This analysis confirmed that there is strong interaction between CTAB and sulfur. FTIR analysis was conducted on sulfur electrodes cycled for 10 and 100 cycles, and the results indicate that the CTAB remains intact after cycling, but with reduced peak intensities (Figure S7).

The cycle life and performance of Li/S cells are often limited by structural degradation and/or failure of the electrodes. Volume expansion/contraction (~76%) during cycling is unavoidable in the sulfur electrode and can result in the electrical isolation of active material (i.e., sulfur) from the current collectors and, therefore, gradual capacity loss during cycling. In this aspect, the binder plays an important role in improving the service life of Li/S cells.<sup>11,37</sup> The essential requirements of an ideal binder include (1) good adhesion to the electrode materials, (2) the ability to create a good electronically conductive network structure between sulfur and conductive carbon, and (3) maintenance of the structural integrity of the electrode during cell operation.<sup>11</sup> Therefore, elastomeric binders are a good choice for maintaining the integrity of the electrode structure during cycling by better accommodating the volume change of the active sulfur component in the electrode. Rubbery materials are unique in that they are both elastic and viscous. Therefore, elastomeric materials have been widely used as shock/vibration isolators or dampers. Elastomeric materials have low elastic modulus and are, therefore, capable of sustaining a deformation of as much as 1000%. SBR is an elastomeric material, and its elongation can be as much as 250–700%. Its Young's modulus is 2–10 MPa, while PVDF's Young's modulus is 2000–2900 MPa, which means that PVDF is much stiffer than SBR. The elongation of PVDF can be only 20–25%. When an elastomeric SBR binder was employed with CMC as the thickening agent, sulfur electrodes showed a much improved cycling performance compared to those with polyethylene oxide (PEO) and PVDF binders.<sup>38</sup>

In this work, the traditional PVDF binder has been replaced with an elastomeric SBR/CMC binder to further improve the cycling performance of CTAB-modified S-GO nanocomposite cathodes. Cyclic voltammetry experiments between 1.5 and 2.8 V vs Li/Li<sup>+</sup> were conducted on CTAB-modified S-GO nanocomposite electrodes made with PVDF and SBR/CMC binders. We intentionally used a very slow scan rate of 10  $\mu\text{V/s}$  (approximately 72 h for 1 cycle between 1.5 and 2.8 V) to obtain a higher utilization of sulfur (i.e., larger volume expansion of sulfur) and allow time for the polysulfide shuttle, if any. Two reduction peaks and one oxidation peak are clearly shown in the cyclic voltammograms (Figure 3a). S-GO nanocomposite cathodes made with PVDF binder showed a decrease in current density of both oxidation and reduction peaks due to the loss of capacity during cycling. Additionally, both oxidation and reduction peaks became broadened to a great extent, indicating that the collection of current had become difficult, which can be attributed to the structural disintegration of electrode (i.e., electrical isolation of sulfur from the current collector) by mechanical degradation.

In contrast, the S-GO nanocomposite electrode made with a SBR/CMC binder showed very stable cyclic voltammograms during 10 cycles under this severe condition, indicating the importance of maintaining intimate contact between the sulfur and carbon during cycling, enabled by the elastomeric binder (Figure 3b). The overlap of the oxidation and reduction peaks and their small separation implies that this electrode can

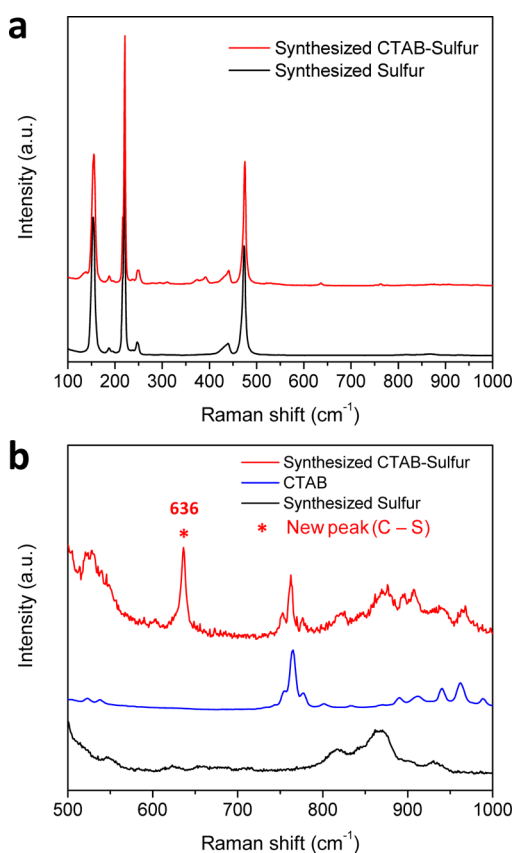


**Figure 2.** Investigation into the interaction between sulfur and CTAB: (a) Raman spectra collected on synthesized sulfur and CTAB-modified sulfur. (b) Enlarged view of Raman spectra on CTAB, synthesized sulfur, and CTAB-modified sulfur from 500 to 1000  $\text{cm}^{-1}$ . It clearly shows the formation of a new peak, which can be assigned as a C-S bond ( $600\text{--}700\text{ cm}^{-1}$ ), confirming that there is strong interaction between CTAB and sulfur.

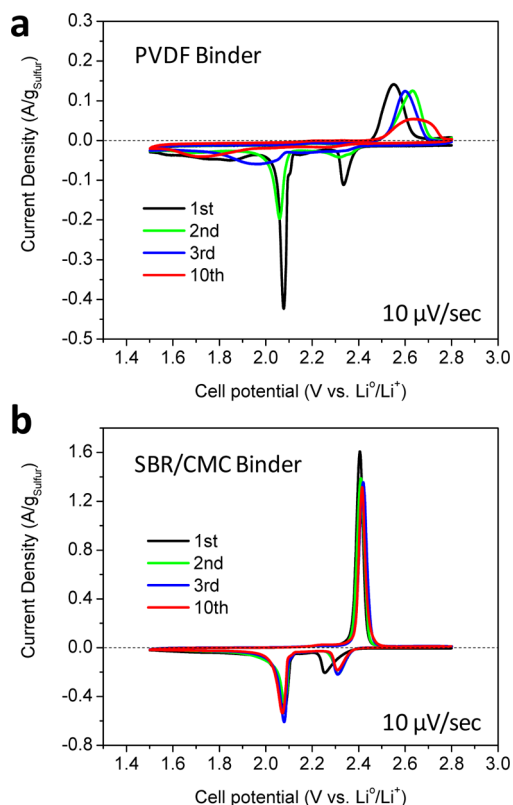


**Figure 3.** Cyclic voltammograms of Li/S cells employing CTAB-modified S–GO nanocomposite electrodes fabricated with different binders: (a) traditional PVDF binder and (b) elastomeric SBR/CMC (1:1 by weight) binder. The S–GO composite contained 80% S. Electrodes made with elastomeric SBR/CMC binder showed much improved cycling performance by mitigating the mechanical degradation of the electrode. This result demonstrates the importance of maintaining intimate contact between the sulfur and carbon during cycling. Cells were cycled between 1.5 and 2.8 V for 10 cycles at the constant scan rate of  $0.01 \text{ mV}\cdot\text{s}^{-1}$ . Cycles 1, 2, 3, and 10 are shown. The current is normalized by the weight of sulfur. 1 M LiTFSI in PYR14TFSI/DOL/DME mixture (2:1:1 by volume) with 0.1 M  $\text{LiNO}_3$  was used as the electrolyte (total  $60 \mu\text{L}$ ).

operate with a very high efficiency, good reversibility, and fast kinetics. In addition to the elastomeric property of the SBR binder, a SBR–CMC mixture was reported to have good adhesion and dispersion capabilities,<sup>39</sup> which also led to the improved performance of CTAB-modified S–GO nanocomposite cathodes. The very sharp peaks and small offset between reduction and oxidation peaks for the SBR–CMC electrode are clear evidence of excellent rate capability.

We also measured the electrochemical impedance spectra of electrodes fabricated with PVDF and SBR based binder after 100 cycles between 1.5 and 2.8 V at rates of 1C and 0.5C for discharge and charge, respectively. We used slower charge rates than discharge rates as we found that how the Li/S cells are charged can significantly influence the cycle life and Coulombic efficiency. We will report these results in a separate publication. As shown in Figure S8, the SBR-containing electrode shows lower charge transfer resistance than the PVDF-based electrode after 100 cycles, clearly indicating that the elastomeric SBR binder helps maintain the integrity of the electrode during cycling.

The principal function of electrolytes for batteries is to provide fast transport of ions between anodes and cathodes. In

Li/S cells, however, there is a major problem with capacity loss during operation, mainly originating from the high solubility of lithium polysulfides in many liquid electrolytes. To address this issue, we introduced a mixture of ionic liquid (PYR14TFSI) and polyethylene glycol dimethyl ether (PEGDME), which led to stable cycling performance.<sup>29</sup> However, the rate capability of Li/S cells with PYR14TFSI/PEGDME-based electrolyte needed to be improved further.

In this work, to improve the rate capability of Li/S cells while maintaining the advantage of using the ionic liquid as effective solvent for minimizing the dissolution of polysulfides, a mixture (1/: v/v) of DOL and DME was introduced to the PYR14TFSI. The electrochemical performance of Li/S cells employing CTAB-modified S–GO nanocomposite cathodes was then evaluated in this new formulation of electrolyte composed of a mixture of PYR14TFSI/DOL/DME (2:1:1 v/v/v) containing 1 M LiTFSI. We also added 0.1 M  $\text{LiNO}_3$  to this electrolyte in order to further minimize polysulfide shuttling by the passivation of the lithium metal surface, as this can prevent chemical reactions of polysulfide species in the electrolyte with the lithium electrodes by preventing polysulfides from directly contacting the lithium metal, thus improving the Coulombic efficiency.<sup>40,41</sup> CTAB-modified S–GO nanocomposite cathodes exhibited a very high reversible capacity of  $1440 \text{ mA}\cdot\text{h/g}$  of sulfur (Figure 4a) and showed a very stable cycling performance up to 40 deep cycles at 0.2C and good rate capability (up to 6C and 3C for discharge and charge, respectively) in this ionic liquid-based novel electrolyte (Figure 4b–d).

We have also performed a cycling test on a Li/S cell employing a CTAB-modified sulfur-graphene oxide nanocomposite electrode with 1 M LiTFSI in DOL/DME (1/1 by volume) with 0.1 M  $\text{LiNO}_3$  without ionic liquid. As shown in Figure S9, a CTAB-modified sulfur-graphene oxide nanocomposite electrode exhibited good cycling performance (e.g.,  $664 \text{ mA}\cdot\text{h/g}$  of sulfur at 1C after 100 cycles) with high Coulombic efficiency (e.g., 96.7% after 100 cycles) in this electrolyte. The demonstrated performance with an electrolyte that does not contain ionic liquid is reasonably good and comparable to those reported by other research groups.<sup>42,43</sup> However, the capacity of the Li/S cells employing CTAB-modified S–GO nanocomposite electrodes but without ionic liquid in the electrolyte started to decay rapidly after 100 cycles, while the Coulombic efficiency was still reasonably good (94.7% after 200 cycles). Further optimization of this electrolyte (e.g., increase of concentration of  $\text{LiNO}_3$  up to 0.2–0.5 M) would be necessary to obtain better cycling performance over more than 100 cycles. When we compare the cycling performance and Coulombic efficiency with those obtained in the ionic liquid based electrolytes, it is clear that the use of the ionic liquid-based electrolyte definitely improves the maintenance of capacity and Coulombic efficiency of the CTAB-modified S–GO nanocomposite cathodes. The ionic liquid (PYR14TFSI) used in this work can also form a passivation layer on the lithium metal surface, and it can further provide some protection of the lithium metal electrode, and thus cycling performance can be further improved. These results clearly support our claims that the CTAB-modified S–GO nanocomposite performs well as a means of stabilizing the S during cell operation, and the use of the ionic-liquid based electrolyte further enhances the cycling stability and Coulombic efficiency. We noted that some unique nanostructures showed good cycling performance without the addition of ionic liquid in the electrolytes,<sup>44,45</sup> and we expect that their performance

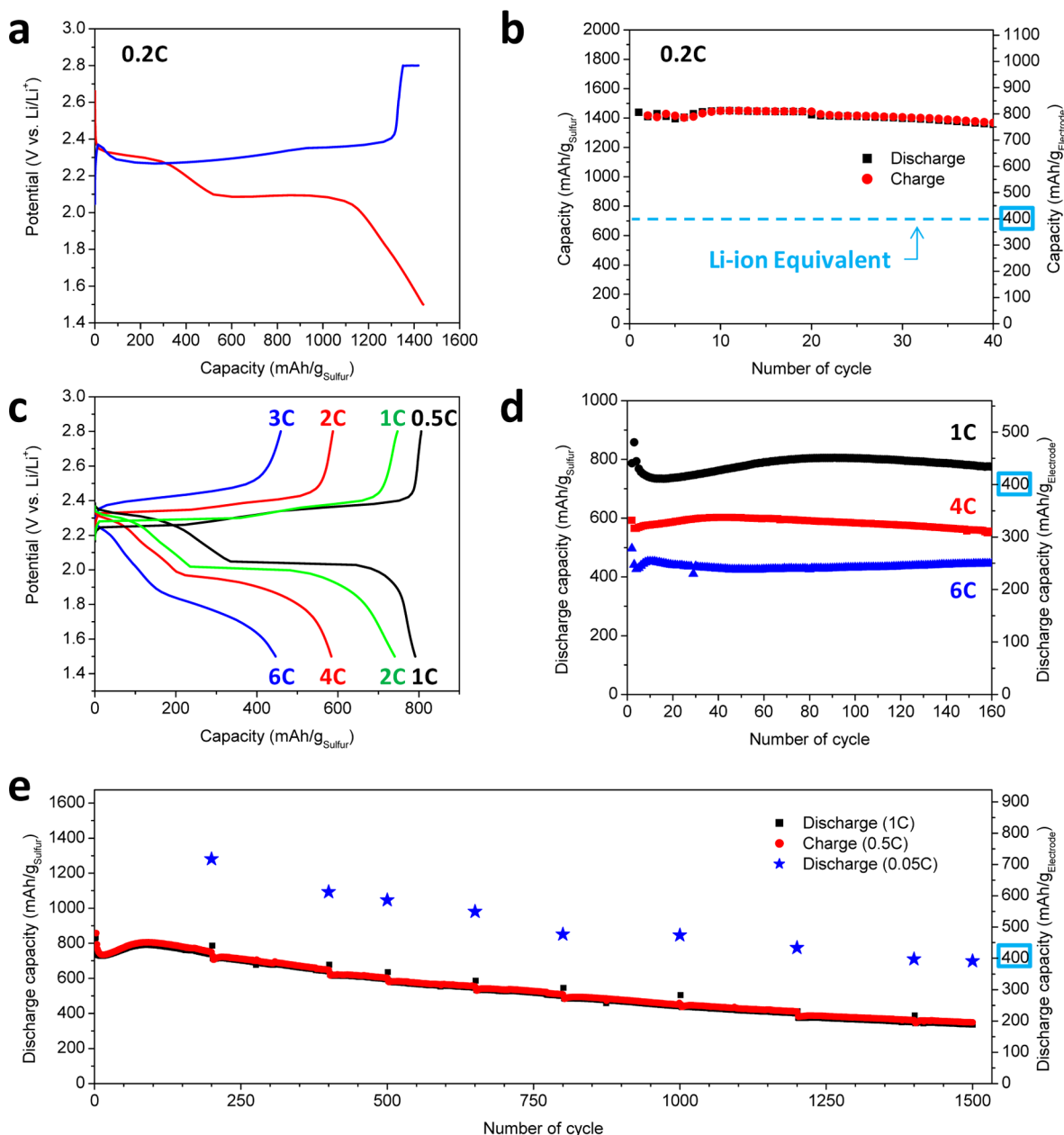


**Figure 4.** Electrochemical performance of Li/S cells employing CTAB-modified S–GO nanocomposite electrodes in a novel ionic liquid-based electrolyte. (a) Initial voltage profiles of Li/S cells cycled at 0.2C showing excellent utilization of sulfur (1C = 1675 mA/g S). (b) Cycling performance of CTAB-modified S–GO composite cathodes at 0.2C for 40 cycles. Capacities are both normalized by the mass of sulfur and total electrode mixture. 400 mA·h/g of electrode is considered to be the Li-ion cell equivalent as typical cathodes for Li-ion cells deliver ~200 mA·h/g of electrode but with higher operating voltage (~4 V) than Li/S cells. This figure shows that CTAB-modified S–GO electrodes can potentially at least double the specific energy of current Li-ion cells. (c) Voltage profiles and (d) cycling performance of CTAB-modified S–GO composite cathodes at different rates. (e) Long-term cycling test results of the Li/S cell with CTAB-modified S–GO composite cathodes. This result represents the longest cycle life (exceeding 1500 cycles) with an extremely low decay rate (0.039% per cycle) demonstrated so far for a Li/S cell. The S–GO composite contained 80% S, and elastomeric SBR/CMC binder was used. 1 M LiTFSI in PYR14TFSI/DOL/DME mixture (2:1:1 by volume) with 0.1 M LiNO<sub>3</sub> was used as the electrolyte (total 60  $\mu$ L).

can be even further improved if they include ionic liquid as demonstrated in this study.

The CTAB-modified S–GO nanocomposite electrode made with a SBR/CMC binder was successfully cycled in the ionic liquid-based electrolyte up to 1500 cycles at rates of 1C and 0.5C for discharge and charge, respectively, with an extremely low capacity decay rate (0.039% per cycle) and high Coulombic efficiency of 96.3% after 1500 cycles (Figure S10). To check the specific capacity that can be obtained at a lower C-rate, cells

were checked periodically during the long-term cycling test, and the discharge/charge capacity was measured using the 0.05C rate. This long-term cycling performance is shown in Figure 4e. After 1000 cycles the discharge capacity was ~846 mA·h/g at 0.05C (Figure S11). This high specific capacity is sufficient to meet the U.S. Department of Energy target for vehicle electrification.<sup>8</sup> Even after 1500 cycles, the discharge capacity was ~700 mA·h/g of sulfur at 0.05C and ~740 mA·h/g of sulfur at 0.02C (Figure S12), showing the great promise of the

unique combination of CTAB-modified S-GO composite, SBR/CMC binder, and PYR14TFSI/DOL/DME/LiNO<sub>3</sub> electrolyte. Recently, a much improved cycle life of Li/S cells has been reported.<sup>44,45</sup> For example, Liu and co-workers reported the excellent cycling performance up to 1500 cycles with 0.043% decay rate per cycle by wrapping graphene over sulfur-coated carbon nanofibers.<sup>44</sup> Cui and co-workers also demonstrated long-cycle performance of Li/S cells up to 1000 cycles with 0.033% decay rate per cycle using sulfur-TiO<sub>2</sub> yolk-shell nanoarchitecture.<sup>45</sup> While it is difficult to compare our performance (e.g., capacities and decay rate) with those measured under different conditions (i.e., voltage range, cycling rates, etc.), successful demonstration of long-term operation up to 1500 cycles with extremely low decay rate of 0.039% per cycle clearly demonstrates the promise of this version of the Li/S cell.

The remaining issue is to achieve an excellent rate capability with good sulfur utilization (i.e., high specific capacity at high C rates). The electrolyte used in this work enabled very high rate operation of Li/S cells up to 6C and 3C for discharge and charge, respectively. An increase in the concentration of LiNO<sub>3</sub> from 0.1 to 0.5 M in PYR14TFSI/DOL/DME (2:1:1 v/v/v) electrolyte was shown to significantly improve the rate capability of Li/S cells (Figure 5). Typical discharge and charge curves are shown in Figure 5a. Even at the 6C rate, very high capacities were obtained and can be maintained for at least 150 cycles with no substantial capacity loss, as shown in Figure 5b. The reversible discharge capacity of Li/S cells with CTAB-modified S-GO composite cathodes in this electrolyte (with 0.5 M LiNO<sub>3</sub>) was ~800 mA·h/g of sulfur at 6C and showed excellent cycling performance with almost 100% Coulombic efficiency after 150 cycles when discharged at 6C and charged at 3C (Figure 5c). We are not aware of any Li/S cells currently showing this high rate capability accompanied by good S utilization. This much-improved rate capability and excellent cycling performance can be attributed to the increased ionic conductivity of the electrolyte and suppressed polysulfide dissolution due to the common ion effect caused by the increased concentration of lithium ions.<sup>46</sup> Other research groups also reported the greatly enhanced sulfur utilization and reduced polysulfide dissolution by increasing the molarity up to 7 M of lithium salt (LiTFSI) in the electrolyte.<sup>47,48</sup> In this work, we used 1 M of LiTFSI but significantly improved the rate capability by increasing the concentration of LiNO<sub>3</sub> up to only 0.5 M, which would be a more commercially viable approach than increasing the expensive LiTFSI concentration in the electrolyte.

It should be noted that a key parameter of a practical cell is the cell-level specific energy.<sup>11</sup> Since the cell's specific energy is largely determined by the sulfur content (%S), sulfur loading (mg/cm<sup>2</sup>), and sulfur utilization (mA·h/g S), it is important to maximize all of these. The estimated cell-level specific energy values (including weight of all cell components except the cell housing) from this work are shown in Figure S13. It is clearly indicated by this graph that high cell-level specific energy can be achieved only when the sulfur content is high, and high utilization is obtained. The initial estimated cell-level specific energy value was ~500 W·h/kg, and even after 1000 cycles, ~300 W·h/kg was estimated, which is much higher than that of currently available Li-ion cells.

In addition to the pre-existing concepts of using elastomeric binders (to mitigate mechanical degradation), ionic-liquid based electrolytes (to minimize the polysulfide shuttle), and

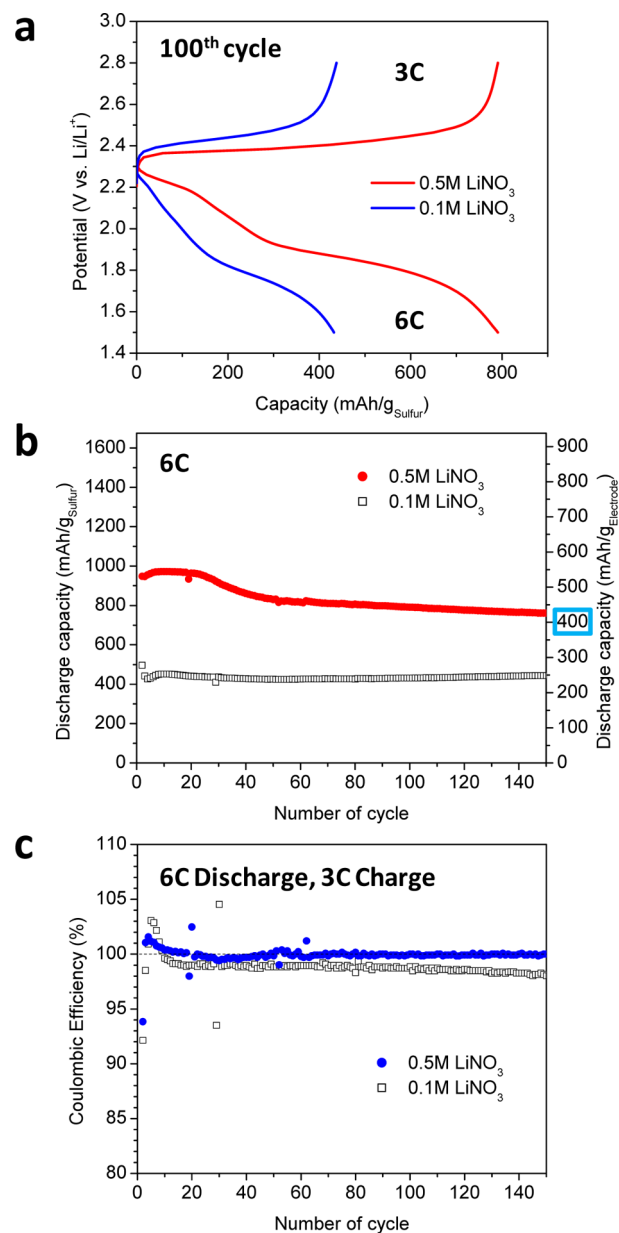


**Figure 5.** Excellent rate capability of Li/S cells enabled by novel ionic liquid-based electrolyte. (a) Voltage profiles of Li/S cells discharged at 6C and charged at 3C showing excellent rate capability. (b) Cycling performance of CTAB-modified S-GO composite cathodes at the 6C rate. (c) Coulombic efficiency of Li/S cells as a function of cycle number. An increase in the concentration of LiNO<sub>3</sub> from 0.1 to 0.5 M in PYR14TFSI/DOL/DME (2:1:1 v/v/v, total 60  $\mu$ L) electrolyte was critical for significantly enhancing the rate capability of Li/S cells with almost 100% Coulombic efficiency achieved after 150 cycles when discharged at 6C and charged at 3C. The S-GO composite contained 80% S, and elastomeric SBR/CMC binder was used.

LiNO<sub>3</sub> as additive (to protect lithium metal electrodes), we further improved the Li/S cell by employing a CTAB-modified S-GO nanocomposite cathode material (to mitigate the loss of sulfur from the electrode by enhancing the absorption capabilities of the active material). The unique combination of all of these concepts in this work has enabled an ultralong life and excellent rate capability, which were not achieved before in Li/S cells.

Another important aspect of this work is the demonstration of the greatly improved cycling ability and the excellent rate capability of lithium metal electrodes when used with these ionic liquid-based electrolytes with a controlled amount of LiNO<sub>3</sub> additive (0.1–0.5 M). The lithium metal electrode has exhibited a cycle life in excess of 1500 cycles with no cell shorting caused by dendrites. This combination of Li metal electrode and ionic liquid-based electrolyte should be compatible with conventional Li-ion cell cathodes such as LiFePO<sub>4</sub> electrodes<sup>49</sup> and may allow the elimination of such materials as carbon or silicon as the negative electrode in Li-ion cells. This can save almost 90% of the weight of the typical carbon negative electrode used in current Li-ion cells.

In summary, we have developed a long-life, high-rate Li/S cell with a high specific energy through a multifaceted approach by uniquely combining CTAB-modified S-GO nanocomposite with an elastomeric SBR/CMC binder and an ionic liquid-based novel electrolyte containing LiNO<sub>3</sub> additive. These Li/S cells exhibited a very high initial discharge capacity of 1440 mA·h/g of sulfur at 0.2C with excellent rate capability of up to 6C for discharge and 3C for charge while still maintaining high specific capacity (e.g., ~800 mA·h/g of sulfur at 6C). We have further demonstrated cycling performance up to 1500 cycles with extremely low decay rate of 0.039% per cycle, which is one of the best performances reported to the best of our knowledge. With the estimated high specific energy, long cycle life, and excellent rate capability demonstrated in this work, the Li/S cell seems to be a promising candidate to challenge the dominant position of the current Li-ion cells.

## ■ ASSOCIATED CONTENT

### 📄 Supporting Information

Experimental details and additional figures. This material is available free of charge via the Internet at <http://pubs.acs.org>.

## ■ AUTHOR INFORMATION

### Corresponding Authors

\*E-mail: [ejcairns@lbl.gov](mailto:ejcairns@lbl.gov).

\*E-mail: [yzgzhang2012@sinano.ac.cn](mailto:yzgzhang2012@sinano.ac.cn).

### Author Contributions

M.-K.S. designed/performed the experiments and analyzed the data. Y.Z. and E.J.C. guided the planning and analyzed and discussed results. M.-K.S., Y.Z., and E.J.C. wrote this paper.

### Notes

The authors declare no competing financial interest.

## ■ ACKNOWLEDGMENTS

This work was supported by University of California, Office of The President, UC Proof of Concept award No. 12PC247581, and by the Office of Science, Office of Basic Energy Sciences, of the U.S. Department of Energy under contract No. DE-AC02-05CH11231.

## ■ REFERENCES

- (1) Armand, M.; Tarascon, J. M. *Nature* **2008**, *451*, 652–657.
- (2) Song, M.-K.; Park, S.; Alamgir, F. M.; Cho, J.; Liu, M. *Mater. Sci. Eng. R* **2011**, *72*, 203–252.
- (3) Scrosati, B.; Hassoun, J.; Sun, Y.-K. *Energy Environ. Sci.* **2011**, *4*, 3287–3295.
- (4) Jung, H. G.; Jang, M. W.; Hassoun, J.; Sun, Y. K.; Scrosati, B. *Nat. Commun.* **2011**, *2*, 516.
- (5) Ellis, B. L.; Lee, K. T.; Nazar, L. F. *Chem. Mater.* **2010**, *22*, 691–714.

- (6) Whittingham, M. S. *MRS Bull.* **2008**, *33*, 411–419.
- (7) Cairns, E. J.; Albertus, P. Batteries for Electric and Hybrid-Electric Vehicles. In *Annual Review of Chemical and Biomolecular Engineering*; Prausnitz, J. M., Doherty, M. F., Segalman, M. A., Eds.; Annual Reviews: Palo Alto, 2010; Vol. 1, pp 299–320.
- (8) Doug, T. *FreedomCAR Program R&D on Energy Storage Systems*; Office of Basic Energy Sciences, U.S. Department of Energy: Washington, DC, 2003.
- (9) Li, W.; Zheng, G.; Yang, Y.; Seh, Z. W.; Liu, N.; Cui, Y. *Proc. Natl. Acad. Sci.* **2013**, *110*, 7148–7153.
- (10) Bruce, P. G.; Freunberger, S. A.; Hardwick, L. J.; Tarascon, J.-M. *Nat. Mater.* **2012**, *11*, 19–29.
- (11) Song, M.-K.; Cairns, E. J.; Zhang, Y. *Nanoscale* **2013**, *5*, 2186–2204.
- (12) Ji, X. L.; Nazar, L. F. *J. Mater. Chem.* **2010**, *20*, 9821–9826.
- (13) Manthiram, A.; Fu, Y.; Su, Y.-S. *Acc. Chem. Res.* **2012**, *46*, 1125–1134.
- (14) Yang, Y.; Zheng, G.; Cui, Y. *Chem. Soc. Rev.* **2013**, *42*, 3018–3032.
- (15) Cai, K.; Song, M.-K.; Cairns, E. J.; Zhang, Y. *Nano Lett.* **2012**, *12*, 6474–6479.
- (16) Yang, Y.; Yu, G. H.; Cha, J. J.; Wu, H.; Vosgueritchian, M.; Yao, Y.; Bao, Z. A.; Cui, Y. *ACS Nano* **2011**, *5*, 9187–9193.
- (17) Zhang, B.; Qin, X.; Li, G. R.; Gao, X. P. *Energy Environ. Sci.* **2010**, *3*, 1531–1537.
- (18) Ji, X.; Evers, S.; Black, R.; Nazar, L. F. *Nat. Commun.* **2011**, *2*, 325.
- (19) Guo, J.; Yang, Z.; Yu, Y.; Abruña, H. c. D.; Archer, L. A. *J. Am. Chem. Soc.* **2012**, *135*, 763–767.
- (20) Mikhaylik, Y. V.; Akridge, J. R. *J. Electrochem. Soc.* **2004**, *151*, A1969–A1976.
- (21) Yang, P. D.; Tarascon, J. M. *Nat. Mater.* **2012**, *11*, 560–563.
- (22) Ji, X.; Lee, K. T.; Nazar, L. F. *Nat. Mater.* **2009**, *8*, 500–506.
- (23) Jayaprakash, N.; Shen, J.; Moganty, S. S.; Corona, A.; Archer, L. A. *Angew. Chem., Int. Ed.* **2011**, *50*, 5904–5908.
- (24) Liang, C. D.; Dudney, N. J.; Howe, J. Y. *Chem. Mater.* **2009**, *21*, 4724–4730.
- (25) Wei, W.; Wang, J. L.; Zhou, L. J.; Yang, J.; Schumann, B.; NuLi, Y. N. *Electrochem. Commun.* **2011**, *13*, 399–402.
- (26) Zheng, G.; Yang, Y.; Cha, J. J.; Hong, S. S.; Cui, Y. *Nano Lett.* **2011**, *11*, 4462–4467.
- (27) Wang, J. L.; Yang, J.; Xie, J. Y.; Xu, N. X.; Li, Y. *Electrochem. Commun.* **2002**, *4*, 499–502.
- (28) Wang, J.; Chew, S. Y.; Zhao, Z. W.; Ashraf, S.; Wexler, D.; Chen, J.; Ng, S. H.; Chou, S. L.; Liu, H. K. *Carbon* **2008**, *46*, 229–235.
- (29) Ji, L.; Rao, M.; Zheng, H.; Zhang, L.; Li, Y.; Duan, W.; Guo, J.; Cairns, E. J.; Zhang, Y. *J. Am. Chem. Soc.* **2011**, *133*, 18522–18525.
- (30) Zhang, L.; Ji, L.; Glans, P.-A.; Zhang, Y.; Zhu, J.; Guo, J. *Phys. Chem. Chem. Phys.* **2012**, *14*, 13670–13675.
- (31) Schwab, G.; Chavany, C.; Duroux, I.; Goubin, G.; Lebeau, J.; Hélène, C.; Saison-Behmoaras, T. *Proc. Natl. Acad. Sci.* **1994**, *91*, 10460–10464.
- (32) Brigger, I.; Dubernet, C.; Couvreur, P. *Adv. Drug Delivery Rev.* **2002**, *54*, 631–651.
- (33) Zhao, X.; Shi, Y.; Cai, Y.; Mou, S. *Environ. Sci. Technol.* **2008**, *42*, 1201–1206.
- (34) Li, J.; Zhao, X.; Shi, Y.; Cai, Y.; Mou, S.; Jiang, G. *J. Chromatogr., A* **2008**, *1180*, 24–31.
- (35) Niu, H.; Cai, Y.; Shi, Y.; Wei, F.; Mou, S.; Jiang, G. *J. Chromatogr., A* **2007**, *1172*, 113–120.
- (36) Khoshnevisan, K.; Barkhi, M.; Zare, D.; Davoodi, D.; Tabatabaei, M. *Synth. React. Inorg., Metal-Org., Nano-Metal Chem.* **2012**, *42*, 644–648.
- (37) Seh, Z. W.; Zhang, Q.; Li, W.; Zheng, G.; Yao, H.; Cui, Y. *Chem. Sci.* **2013**, *5*, 3673–3677.
- (38) Rao, M.; Song, X.; Liao, H.; Cairns, E. J. *Electrochim. Acta* **2012**, *65*, 228–233.
- (39) He, M.; Yuan, L. X.; Zhang, W. X.; Hu, X. L.; Huang, Y. H. *J. Phys. Chem. C* **2011**, *115*, 15703–15709.

- (40) Aurbach, D.; Pollak, E.; Elazari, R.; Salitra, G.; Kelley, C. S.; Affinito, J. J. *Electrochem. Soc.* **2009**, *156*, A694–A702.
- (41) Zhang, S. S. *Electrochim. Acta* **2012**, *70*, 344–348.
- (42) Zu, C.; Su, Y.-S.; Fu, Y.; Manthiram, A. *Phys. Chem. Chem. Phys.* **2013**, *15*, 2291–2297.
- (43) Fu, Y.; Su, Y. S.; Manthiram, A. *Adv. Energy Mater.* **2013**, DOI: 10.1002/aenm.201300655.
- (44) Lu, S.; Cheng, Y.; Wu, X.; Liu, J. *Nano Lett.* **2013**, *13*, 2485–2489.
- (45) Seh, Z. W.; Li, W.; Cha, J. J.; Zheng, G.; Yang, Y.; McDowell, M. T.; Hsu, P.-C.; Cui, Y. *Nat. Commun.* **2013**, *4*, 1331.
- (46) Shin, E. S.; Kim, K.; Oh, S. H.; Cho, W. I. *Chem. Commun.* **2013**, *49*, 2004–2006.
- (47) Suo, L.; Hu, Y.-S.; Li, H.; Armand, M.; Chen, L. *Nat. Commun.* **2013**, *4*, 1481.
- (48) Lee, J.; Zhao, Y.; Thieme, S.; Kim, H.; Oschatz, M.; Borchardt, L.; Magasinski, A.; Cho, W.; Kaskel, S.; Yushin, G. *Adv. Mater.* **2013**, *25*, 4573–4579.
- (49) Shin, J. H.; Basak, P.; Kerr, J. B.; Cairns, E. J. *Electrochim. Acta* **2008**, *54*, 410–414.

Supplementary Information

**A long-life, high-rate lithium/sulfur cell: a multi-faceted  
approach to enhancing cell performance**

Min-Kyu Song<sup>1,2</sup>, Yuegang Zhang<sup>1,3\*</sup> and Elton J. Cairns<sup>2,4\*</sup>

<sup>1</sup> The Molecular Foundry, Lawrence Berkeley National Laboratory, Berkeley, CA 94720, USA

<sup>2</sup> Department of Chemical and Biomolecular Engineering, University of California, Berkeley, CA 94720, USA

<sup>3</sup> *i-LAB*, Suzhou Institute of Nano-Tech and Nano-Bionics, Chinese Academy of Sciences, Suzhou 215123, China

<sup>4</sup> Environmental Energy Technologies Division, Lawrence Berkeley National Laboratory, Berkeley, CA 94720, USA

## Methods

### Synthesis of CTAB-modified S-GO nanocomposites.

0.58g of sodium sulfide ( $\text{Na}_2\text{S}$ , anhydrous, Alfa Aesar) was dissolved in 25ml ultrapure water (Millipore) to form a  $\text{Na}_2\text{S}$  solution, then 0.72g elemental sulfur (S, sublimed, 99.9%, Mallinckrodt) was added to the  $\text{Na}_2\text{S}$  solution and stirred with a magnetic stirrer for 2 hours at room temperature. The color of the solution changed slowly from yellow to orange as the sulfur dissolved. After dissolution of the sulfur, a sodium polysulfide ( $\text{Na}_2\text{S}_x$ ) solution was obtained. Commercial graphene oxide (GO) water dispersion (10mg/ml, ACS Material) was used for the deposition of S onto GO by a chemical precipitation method in an aqueous solution. 18ml of GO solution was taken by an auto pipette and diluted with ultrapure water (162ml) to form a GO suspension (180mg of GO in 180ml of ultrapure water). Different amounts (0~5mM) of cetyltrimethyl ammonium bromide (CTAB,  $\text{CH}_3(\text{CH}_2)_{15}\text{N}(\text{Br})(\text{CH}_3)_3$ , Sigma Aldrich) were added to the GO suspension and stirred for 2 hours. Then, the  $\text{Na}_2\text{S}_x$  solution was added to the prepared GO-CTAB blended solution drop-wise using a glass pipette while stirring. Then, the  $\text{Na}_2\text{S}_x$ -GO-CTAB blended solution was stirred for 16 hours (overnight). Next, the as-prepared  $\text{Na}_2\text{S}_x$ -GO-CTAB blended solution was slowly added to 100ml of 2M formic acid ( $\text{HCOOH}$ , 88%, Aldrich) using a burette while stirring. The resulting mixture was stirred for 0.5 hours or 2 hours for elemental S to be precipitated onto the GO. Finally, the CTAB-modified S-GO composite was filtered and washed with acetone and ultrapure water several times to remove salts and impurities. Then, the CTAB-modified S-GO composite was dried at  $50^\circ\text{C}$  in a vacuum oven for 24 hours. The as-synthesized CTAB-modified S-GO composite was heat-treated in a tube furnace under flowing argon with a controlled flow rate of 100cc/s at  $155^\circ\text{C}$  for 12 hours. In order to control the S content, 0.5hours was also used.

### Materials characterization.

A scanning electron microscope (SEM, Zeiss Gemini Ultra-55) was operated at an accelerating voltage of 3 kV to examine the morphology of the CTAB-modified S-GO nanocomposites. An energy dispersive X-ray spectrometer attached to the SEM (JEOL JSM-7500F) was used to conduct elemental analysis of sulfur and the distribution with an accelerating voltage of 10 kV. Thermogravimetric analysis (TGA, TA Instruments Q5000) was used to determine the weight of the S on the GO using a heating rate of  $10^\circ\text{C}/\text{min}$  in  $\text{N}_2$ . Fourier transform infrared spectroscopy (FT-IR, PerkinElmer Spectrum One) was used to examine the presence of CTAB on the S-GO surface. Raman spectroscopy (Horiba LabRAM ARAMIS) was used to investigate the interaction between CTAB and sulfur.

### **Cell assembly and electrochemical characterization.**

The sulfur electrodes were fabricated by mixing the S-GO nanocomposite, carbon black (Super P) with a binder (either PVDF or SBR/CMC 1:1 by weight) at a weight ratio of 70:20:10 in N-methyl-2-pyrrolidone (NMP) solvent for PVDF or ethanol/water (1:1 by volume) solution for SBR/CMC to form a slurry using an ultrasonicator. The resulting slurry was uniformly spread via a doctor blade (Elcometer 3540 Bird Film Applicator) on pure aluminum foil. The solvent was allowed to evaporate at room temperature for 24 hours. The electrodes were then dried in a vacuum oven at 50°C for 48 hours to fully eliminate any solvent residue. The electrode was punched into circular pieces with a diameter of 12.7 mm for cell assembly. The average sulfur loading of the electrodes was  $\sim 0.8\text{mg/cm}^2$ .

For the electrolyte, 1 mol/kg lithium bis(trifluoromethylsulfonyl)imide (LiTFSI, Sigma-Aldrich) in (n-methyl-(n-butyl) pyrrolidinium bis(trifluoromethanesulfonyl)imide (PYR14TFSI, Sigma-Aldrich)/polyethylene glycol dimethyl ether (PEGDME, Sigma-Aldrich) mixture (1:1, by weight) was prepared and used for evaluation of the electrochemical performance of electrodes with different sulfur loadings, CTAB amounts, and heat-treatments. For the long-term cycling test and rate capability measurements, a mixture of 1,3-dioxolane (DOL) and dimethoxyethane (DME) was introduced to PYR14TFSI to form 1 M LiTFSI in PYR14TFSI/DOL/DME mixture (2:1:1 by volume). 0.1M or 0.5M  $\text{LiNO}_3$  was used as an additive in the electrolyte.

CR2032-type coin cells were assembled by sandwiching two separators (Celgard 2400) between a lithium metal foil (99.98%, Cyprus Foote Mineral) and a sulfur electrode fabricated with the S-GO composite in a glove box filled with high-purity argon gas. Cyclic voltammetry was performed using a potentiostat (Biologic VSP) with a voltage range of 1.5 to 2.8V for 10 cycles at a constant scan rate of  $0.01\text{ mVs}^{-1}$ . Galvanostatic discharge and charge testing of the coin cells was performed using a battery cycler (Maccor Series 4000) at different rates between 1.5 and 2.8V. The cell capacity was normalized both by the weight of sulfur and total electrode weight. Electrochemical impedance spectroscopy was performed with amplitude of 5mV in the 1 MHz to 0.1Hz frequency range on a Maccor battery cycler to monitor how the impedance changed during cycling. Before all electrochemical characterizations, the cells were held at open circuit at room temperature for 24 h. All electrochemical characterizations were performed inside a chamber (TestEquity TEC1) maintained at 30 °C.

## Supplementary Discussion

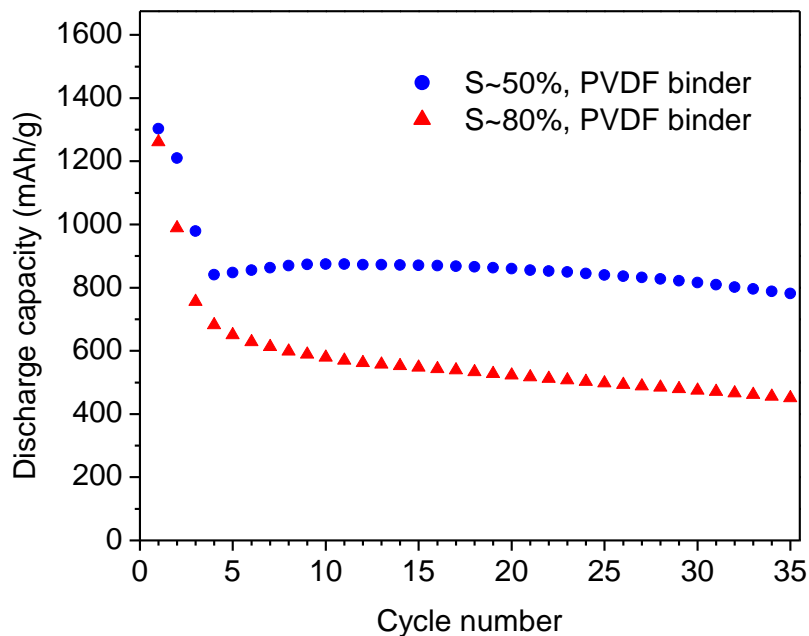


**Figure S1.** Cycling performance of Li/S cells fabricated with S-GO composites of different sulfur content: 50 wt.% and 80 wt.% of sulfur in the S-GO composites. Cells were cycled at a constant current rate of 0.1C after two cycles at 0.02C. PVDF binder was used to fabricate composite S-GO cathodes. The capacity is normalized by the weight of sulfur only. The average sulfur loading of the electrodes is  $0.8\text{mg}/\text{cm}^2$ . For the electrolyte, 1 mol/kg LiTFSI in PYR14TFSI/PEGDME mixture (1:1 by weight) was used.

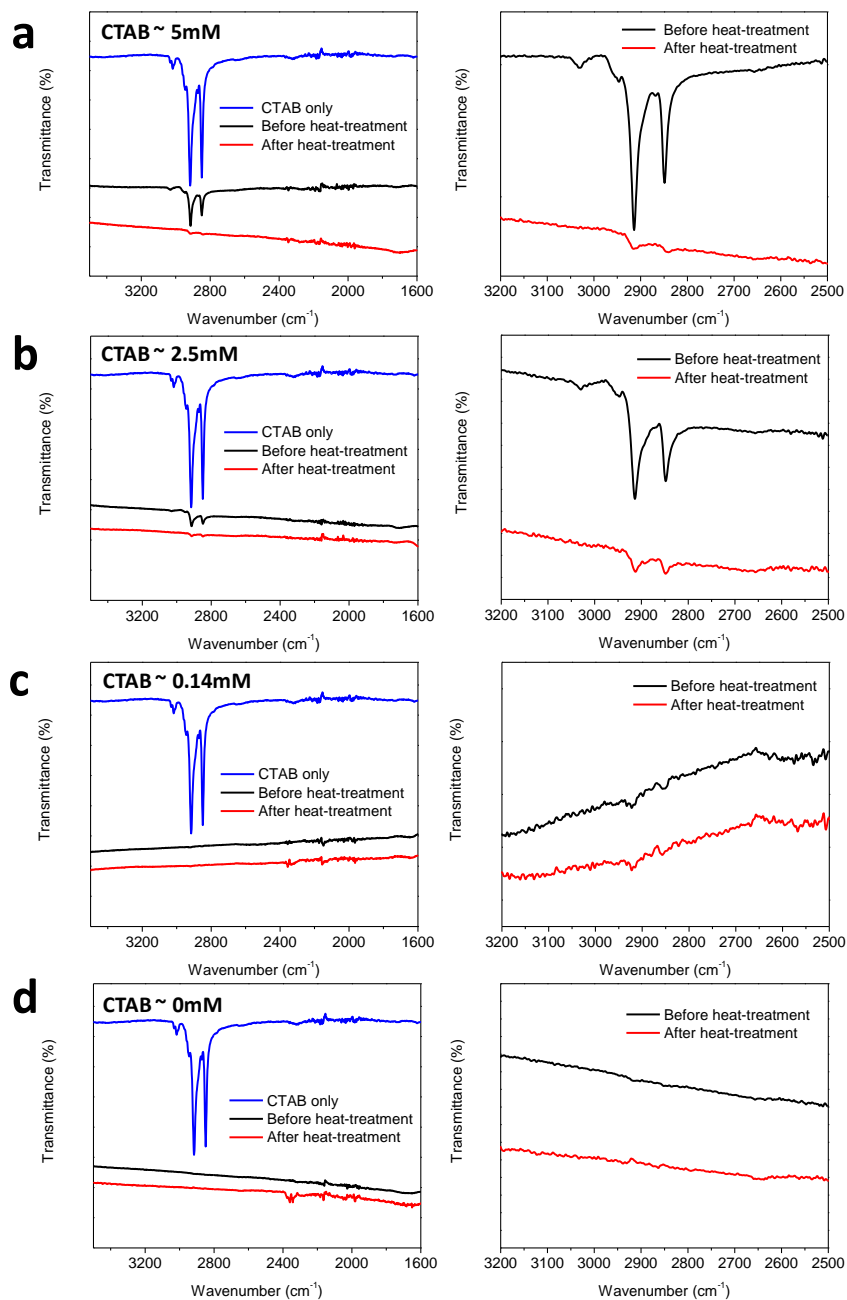


**Figure S2.** FT-IR spectra of S-GO nanocomposites prepared (a) with 5mM CTAB, (b) 2.5mM CTAB, (c) 0.14mM CTAB and (d) without CTAB. The figures on the right side show an enlarged view of the FTIR spectra between 3200 and 2500  $\text{cm}^{-1}$  for the figures on the left side. The peaks at 2918 and 2848  $\text{cm}^{-1}$  can be attributed to two different C-H vibrational bands of CTAB. Figure S2 shows that the S-GO surface was well modified with CTAB.

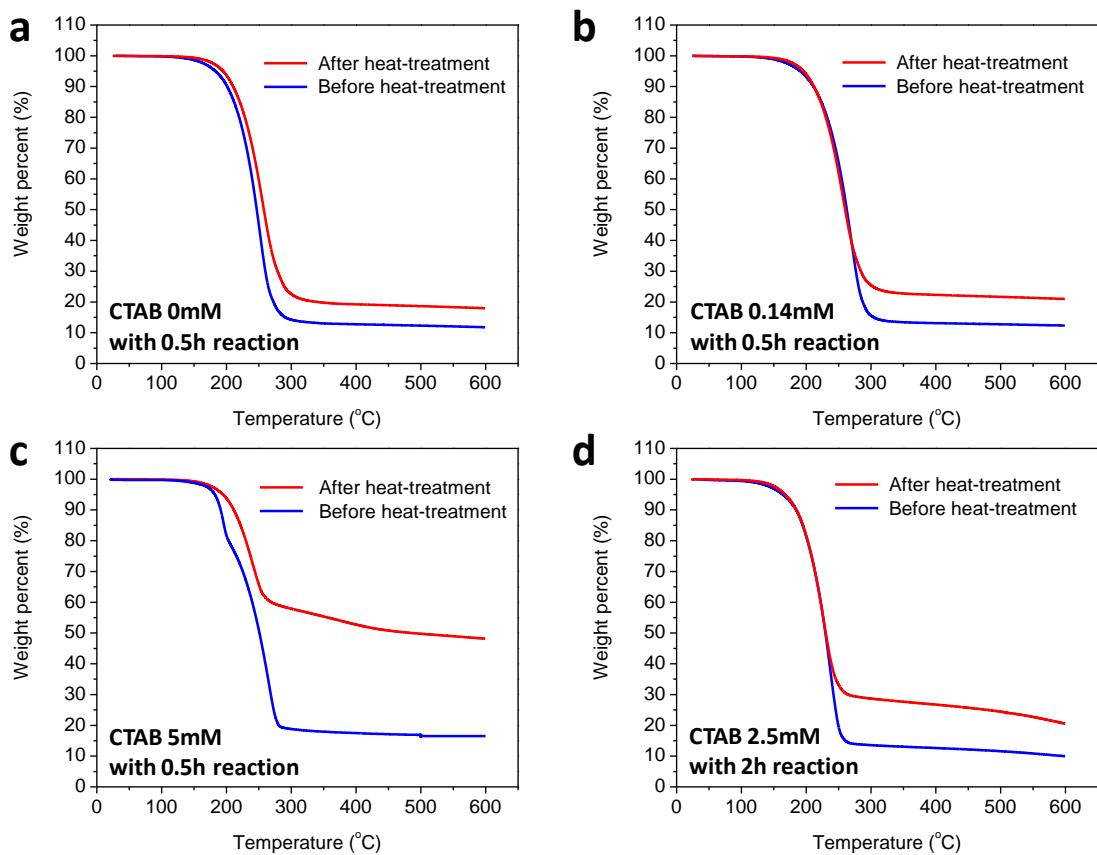


**Figure S3.** TGA curves of S-GO nanocomposites prepared with different amounts of CTAB before and after heat-treatment at 155°C for 12 h in Ar. The deposition time was 30 minutes for samples (a~c) and 2 hours for sample (d).

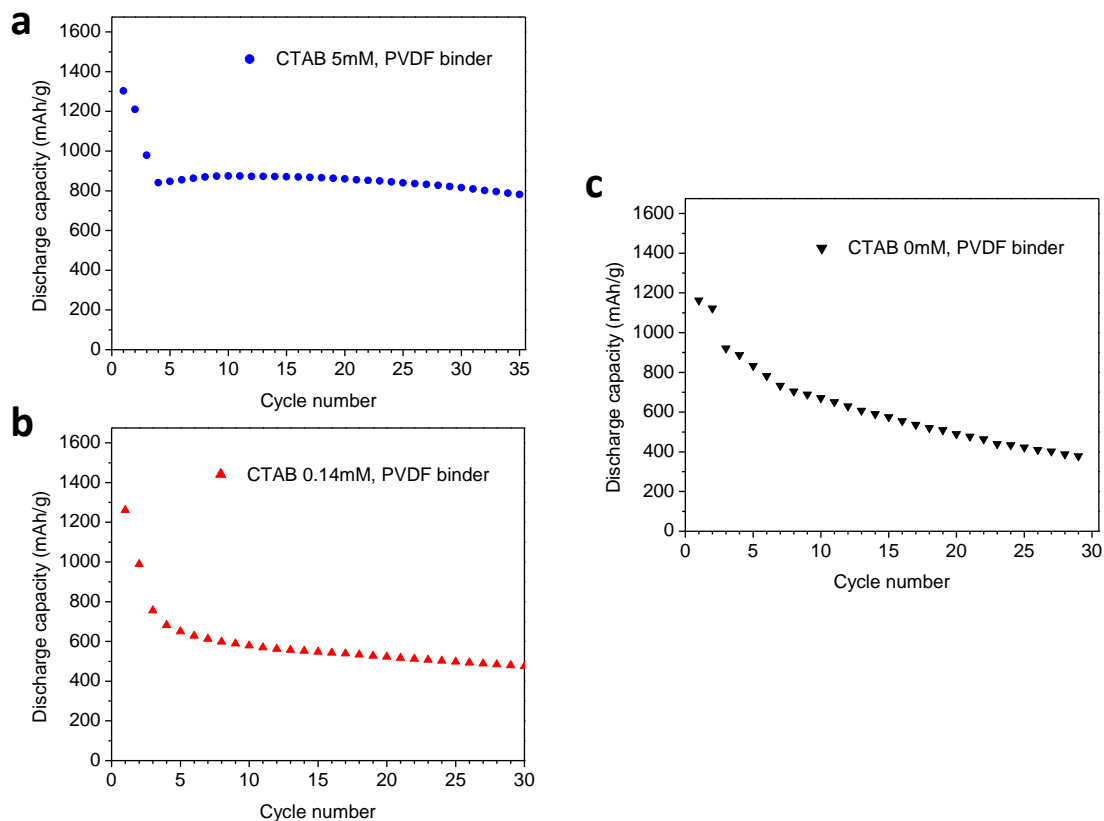


**Figure S4.** Cycling performance of Li/S cells fabricated with S-GO composites prepared with different amounts of CTAB added during the synthesis of S-GO nanocomposites: (a) CTAB ~ 5mM, (b) CTAB ~ 0.14mM, and (c) no CTAB. Cells were cycled at a constant current rate of 0.1C after two cycles at 0.02C. PVDF binder was used to fabricate the composite S cathodes. The capacity is normalized by the weight of sulfur only. For the electrolyte, 1 mol/kg LiTFSI in PYR14TFSI/PEGDME mixture (1:1 by weight) was used.

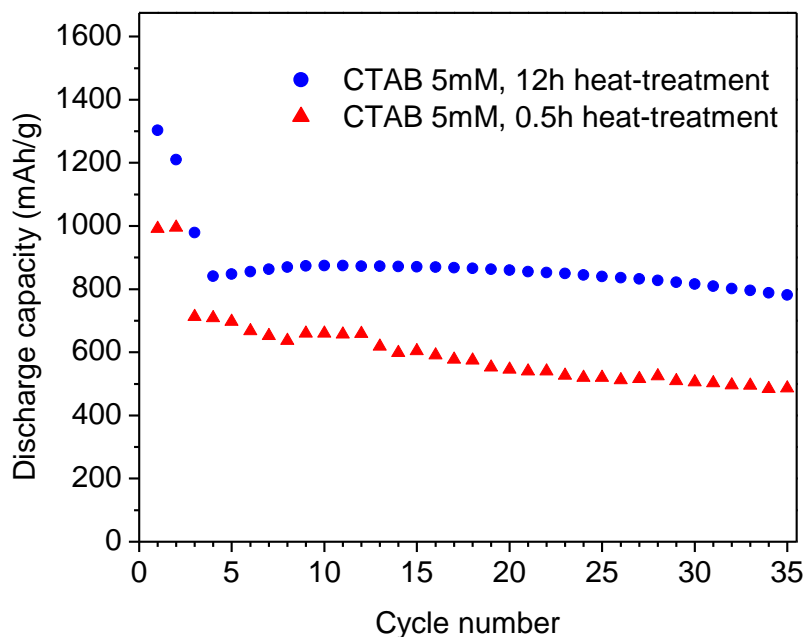


**Figure S5.** Cycling performance of Li/S cells fabricated with S-GO composites prepared with different heat-treatment time (12 hours and 0.5 hours) under Ar atmosphere at 155°C. Cells were cycled at a constant current rate of 0.1C after two cycles at 0.02C. PVDF binder was used to fabricate these composite S cathodes. The capacity is normalized by the weight of sulfur only. The average sulfur loading of the electrodes is 0.8mg/cm<sup>2</sup>. For the electrolyte, 1 mol/kg LiTFSI in PYR14TFSI/PEGDME mixture (1:1 by weight) was used.

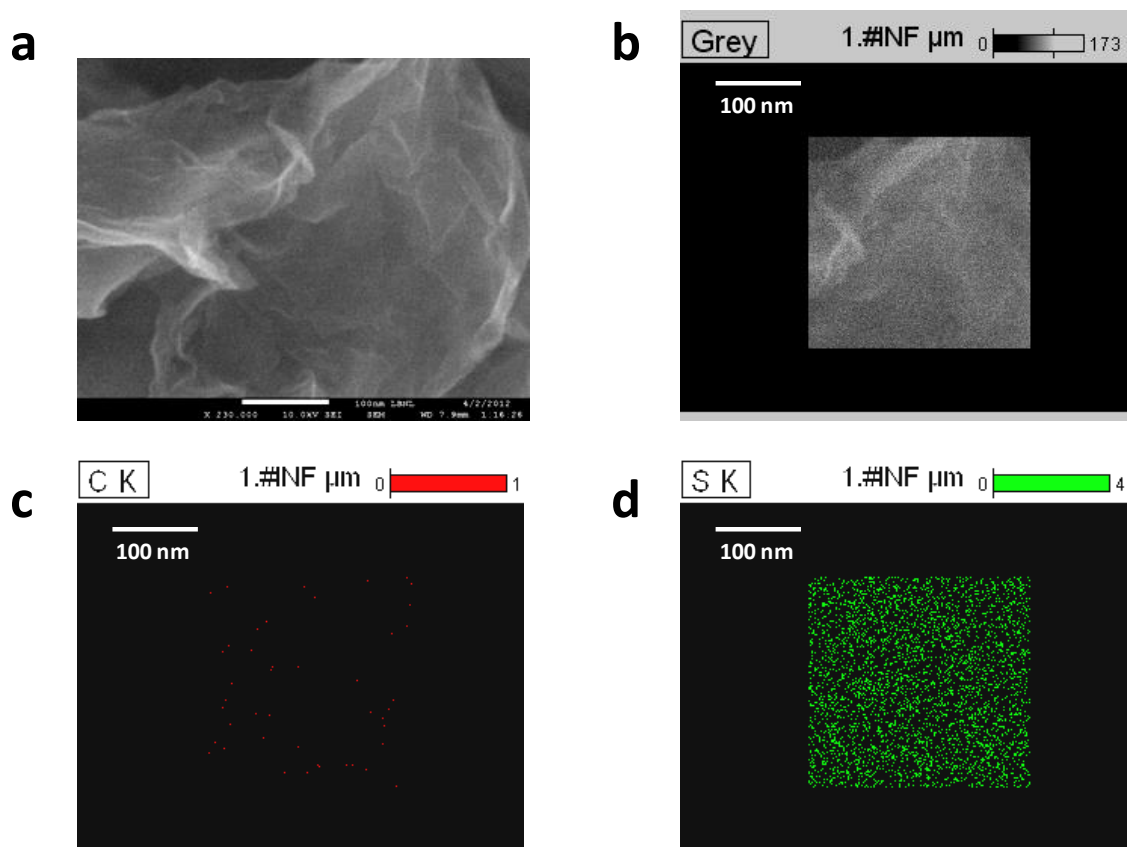


**Figure S6.** (a) SEM image, (b) a selected area for elemental mapping of (c) carbon and (d) sulfur by energy dispersive X-ray spectroscopy of S-GO nanocomposites with 80% sulfur loading.

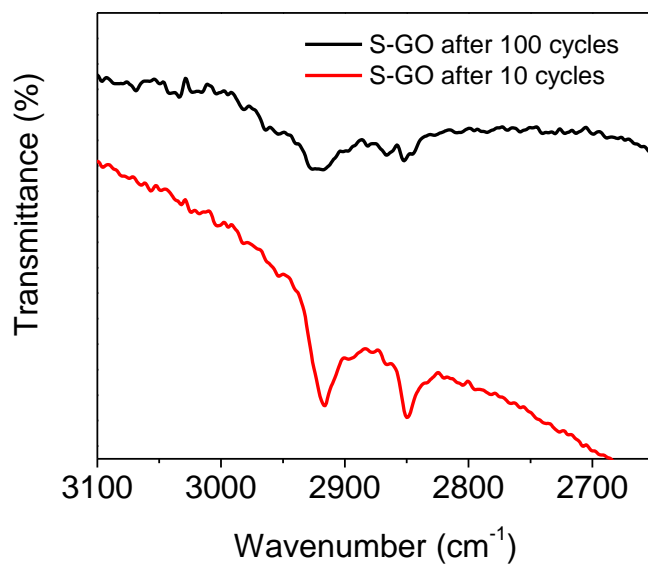


**Figure S7.** FT-IR spectra of S-GO nanocomposites after 10 and 100 cycles. The peaks at 2918 and 2848 cm<sup>-1</sup> can be attributed to two different C-H vibrational bands of CTAB. Figure S7 shows that CTAB remains intact with reduced peak intensities after cycling.

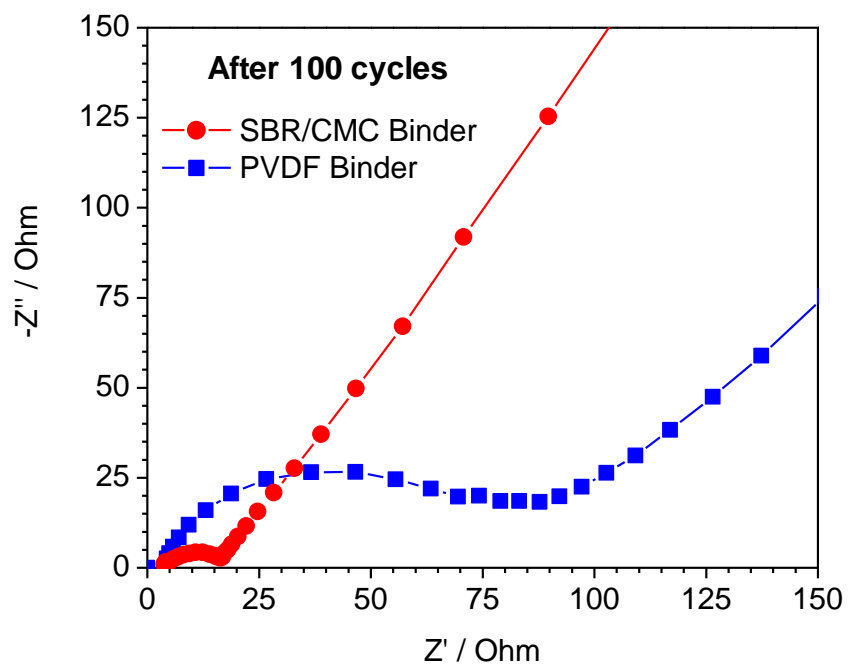


**Figure S8.** Electrochemical impedance spectra (EIS) collected on electrodes fabricated with PVDF and SBR/CMC binder after 100 cycles between 1.5 and 2.8V at rates of 1C and 0.5C for discharge and charge, respectively. The diameter of the semicircle represents the charge transfer resistance at interface. These spectra were measured at fully charged state.

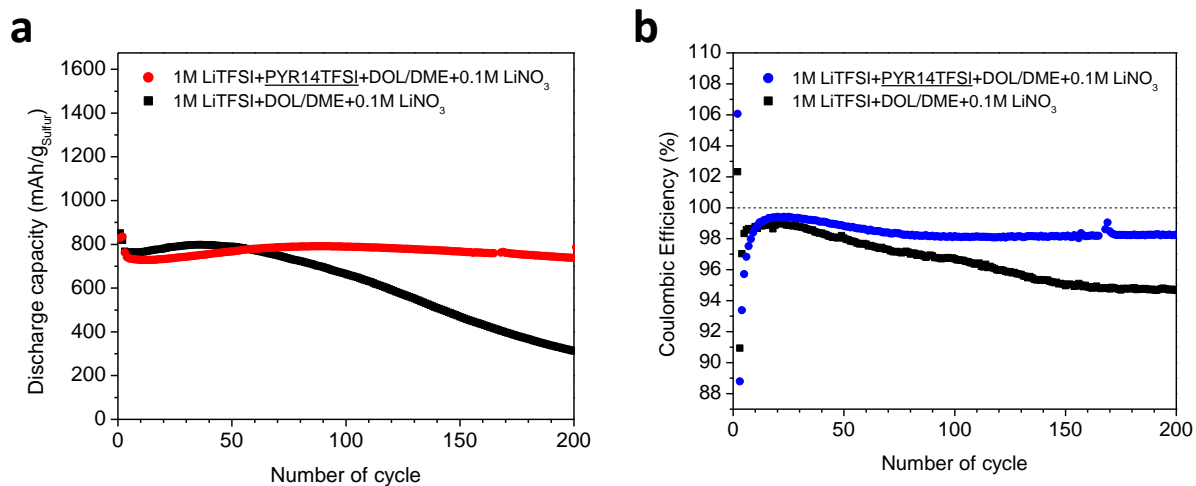


**Figure S9.** Comparison of electrochemical performance up to 200 cycles for Li/S cells employing CTAB-modified S-GO nanocomposite electrodes with and without ionic liquid (PYR14TFSI) in 1M LiTFSI in DOL/DME (1/1 by volume) with 0.1M LiNO<sub>3</sub>. (a) Cycling performance of CTAB-modified S-GO composite cathodes at rates of 1C and 0.5C for discharge and charge, respectively. (b) Coulombic efficiency of Li/S cells as a function of cycle number. The S-GO composite contained 80% S and elastomeric SBR/CMC binder was used.

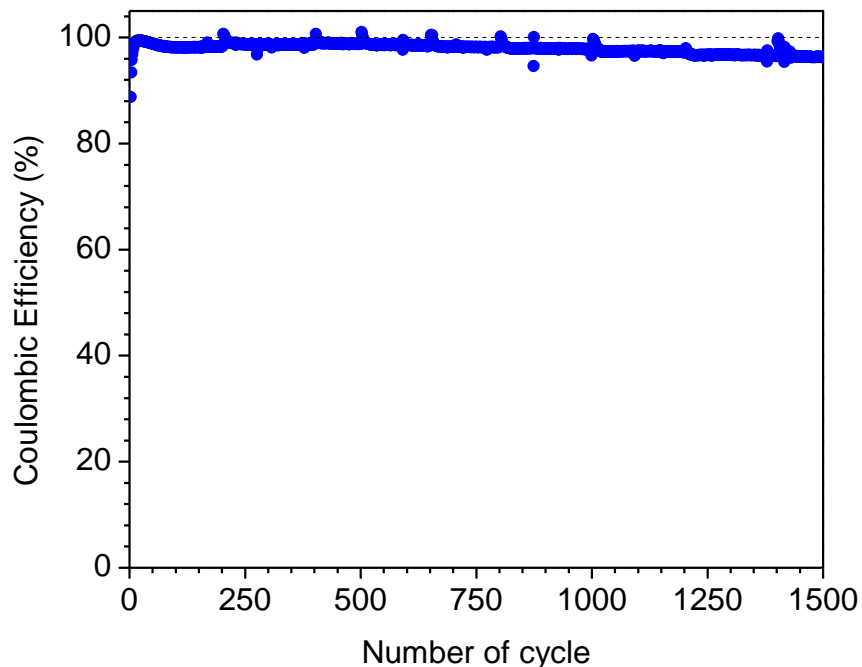


**Figure S10.** Coulombic efficiency of Li/S cells as a function of cycle number. Coulombic efficiencies were 98.8%, 97.8% and 96.3% after 500, 1000, and 1500 cycles at rates of 1C and 0.5C for discharge and charge, respectively. SBR/CMC binder was used to fabricate these composite S-GO cathodes. The S-GO composite contained 80% S, and the electrode composition was 70% S-GO, 20% Super P, and 10% SBR/CMC. For the electrolyte, 1 M LiTFSI in PYR14TFSI/DOL/DME mixture (2:1:1 by volume) with 0.1M LiNO<sub>3</sub> was used.

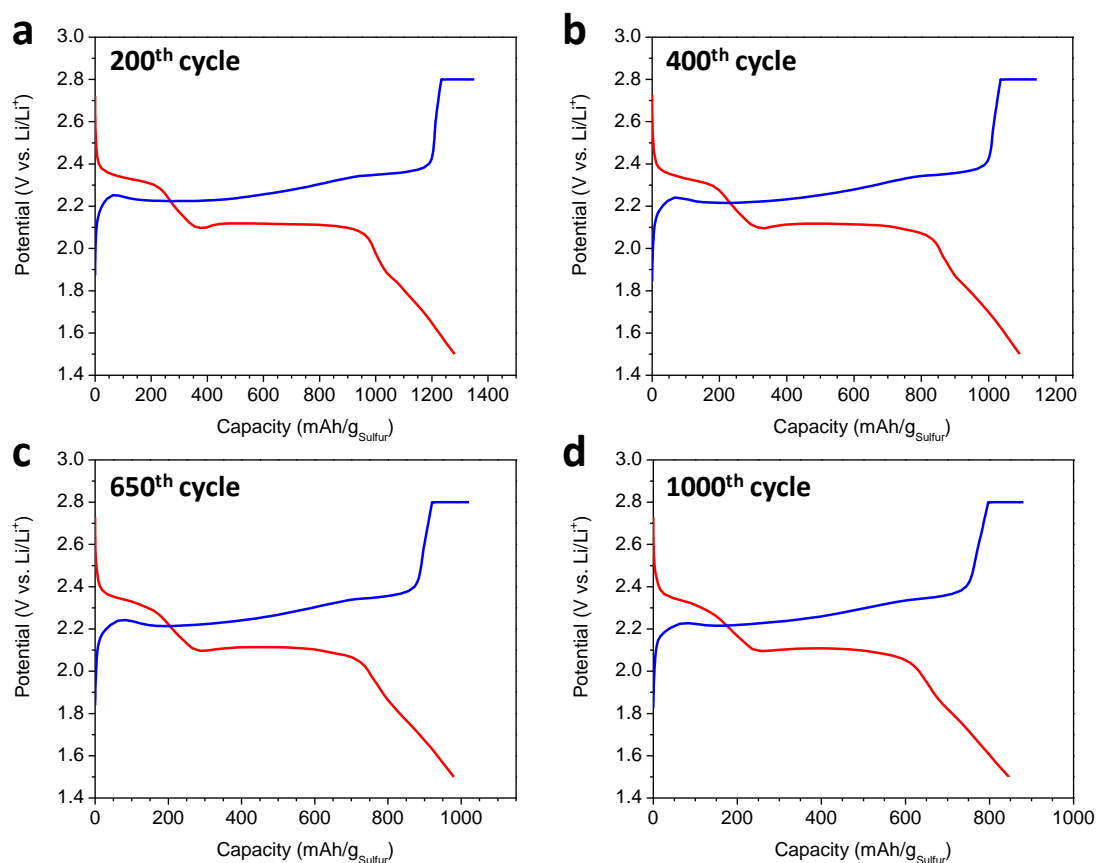


**Figure S11.** Voltage profiles of CTAB-modified S-GO nanocomposite cathodes, cycled between 1.5 and 2.8V at a constant rate of 0.05C after (a) 200 cycles, (b) 400 cycles, (c) 650 cycles, and (d) 1000 cycles at 1C for discharging and 0.5C for charging. Constant voltage was applied after constant current charging until the current drops below 5% of the initial charging current. SBR/CMC binder was used to fabricate these composite S cathodes. The S-GO composite contained 80% S, and the electrode composition was 70% S-GO, 20% Super P, and 10% SBR/CMC. The capacity is normalized by the weight of sulfur only. The average sulfur loading of the electrodes is  $0.8\text{mg}/\text{cm}^2$ . For the electrolyte, 1 M LiTFSI in PYR14TFSI/DOL/DME mixture (2:1:1 by volume) with 0.1M  $\text{LiNO}_3$  was used.

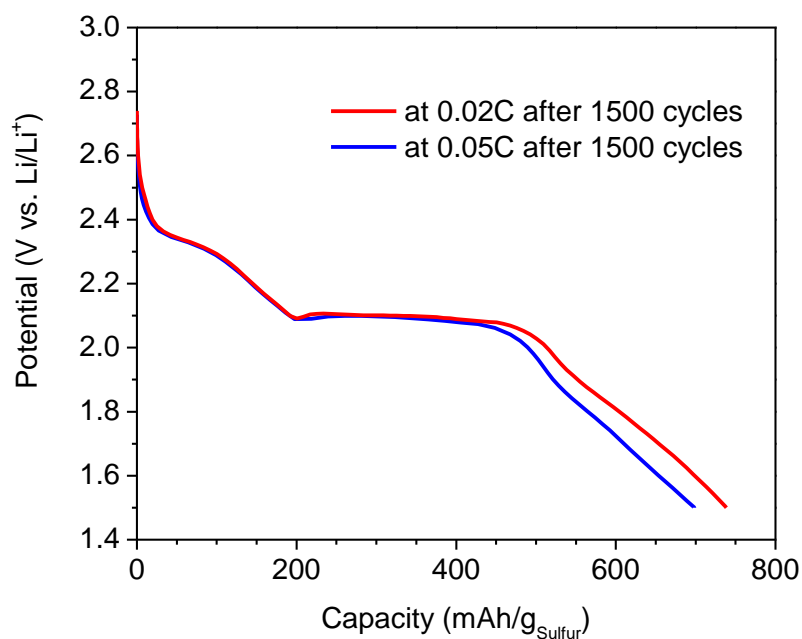


**Figure S12.** Discharge voltage profiles of CTAB-modified S-GO nanocomposite cathodes, cycled between 1.5 and 2.8V at constant rates of 0.02C and 0.05C after 1500 cycles at the 1C rate for discharging and 0.5C rate for charging. SBR/CMC binder was used to fabricate the composite S cathodes. The S-GO composite contained 80% S, and the electrode composition was 70% S-GO, 20% Super P, and 10% SBR/CMC. The capacity is normalized by the weight of sulfur only. The average sulfur loading of the electrodes is 0.8mg/cm<sup>2</sup>. For the electrolyte, 1 M LiTFSI in PYR14TFSI/DOL/DME mixture (2:1:1 by volume) with 0.1M LiNO<sub>3</sub> was used.

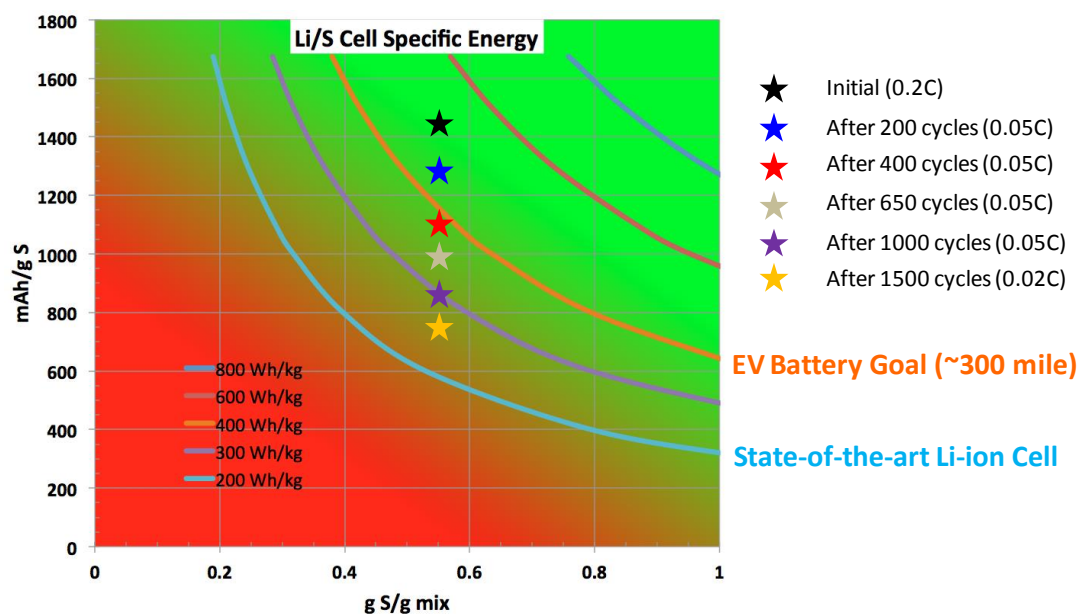
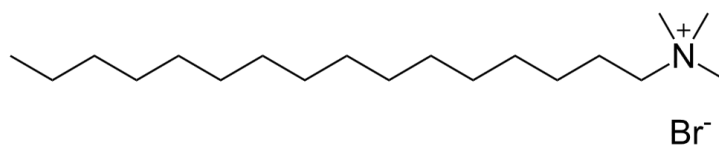
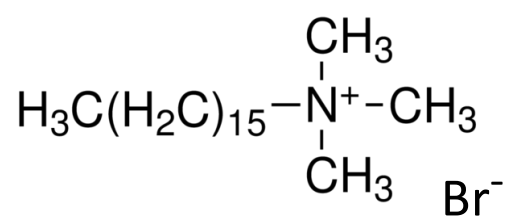


**Figure S13.** Estimated cell-level specific energy plot. Cell specific energy curves are estimated using the weight of all components except the cell housing and shown as a function of the specific capacity and content of sulfur in the electrode. The data of this work is indicated by the solid stars. Details of the calculation are provided in Table S1.

**Table S1.** Data for estimation of the Li/S cell-level specific energy

<b>Design Parameters for Calculations of Cell Specific Energy</b>	
Cell part	Weight of Material for Li/S cell (mg/cm <sup>2</sup> )
Cu Foil (5 microns thick)	4.5
Lithium Electrode (100% excess)	3.6
Electrolyte and separator (50 microns thick)	5
S Electrode (including binder/additives)	6
Al Foil (5 microns thick)	1.4
Total weight	20.5

Cell design parameters used to estimate the cell-level specific energy (including all components except cell-housing) are shown in Table S1. A sulfur electrode loading of 6 mg/cm<sup>2</sup> is assumed to calculate the cell specific energy curves shown in Figure 5. A 100% excess of lithium is assumed with respect to the theoretical amount required for the full conversion of S to Li<sub>2</sub>S. For the electrolyte, two layers of separator (polypropylene, porosity 50%, density = 0.9 g/cm<sup>3</sup>) and organic solvent (average density = 1.1 g/cm<sup>3</sup>) are assumed.



**Scheme S1.** Molecular structure of cetyltrimethyl ammonium bromide (CTAB)